The 9th International Supercritical CO_2 Energy Technologies Symposium
March 2 - 5, 2026, Pittsburgh, PA

Paper #009

Near Carbon-Neutral Power Generation by DME in sCO_2 Oxy-Combustion Cycles

Ghadi Abi Haidar
Research Assistant
Forschungszentrum Jülich
Jülich, Germany
g.abi.haidar@fz-juelich.de

Johanna Leutner
Student
Forschungszentrum Jülich / RWTH Aachen
Jülich/Aachen, Germany
j.leutner@fz-juelich.de

Philipp Morsch
Team Lead
Forschungszentrum Jülich
Jülich, Germany
p.morsch@fz-juelich.de

Prof. Dr.-Ing. Andreas Peschel
Director INW-4
Forschungszentrum Jülich / RWTH Aachen
Jülich/Aachen, Germany
a.peschel@fz-juelich.de

Ghadi Abi Haidar is a mechanical engineering graduate from the University of Kassel-Germany. He is currently a Ph.D. student in process and energy engineering at Forschungszentrum Jülich's Institute for Sustainable Hydrogen Economy - Process and Plant Engineering for Chemical Hydrogen Storage (INW-4). His research focuses on the modeling and simulation of advanced semi-closed sCO_2 oxy-combustion power cycles with dimethyl ether (DME) as fuel.

Johanna Leutner received her M.Sc. in Business Administration and Mechanical Engineering from RWTH Aachen University, specializing in energy engineering. Her Master's thesis, conducted at Forschungszentrum Jülich's Institute for Sustainable Hydrogen Economy (INW-4), focused on the modeling and simulation of combined cycle gas turbines fueled with dimethyl ether (DME).

Philipp Morsch leads the team 'System Integration' at Forschungszentrum Jülich's Institute for Sustainable Hydrogen Economy - Process and Plant Engineering for Chemical Hydrogen Storage (INW-4). His research focuses on integrating hydrogen carriers into industrial applications. Earlier in his career, he was a research assistant at RWTH Aachen University's Chair of High Pressure Gas Dynamics and Shock Wave Laboratory, where he contributed to several publications concerning reaction kinetics and sustainable fuels.

Andreas Peschel is Director for Process and Plant Engineering for Chemical Hydrogen Storage at the Institute for a Sustainable Hydrogen Economy of Forschungszentrum Jülich and a Full Professor at RWTH Aachen University. His primary research activity focuses on innovative process and plant engineering for chemical hydrogen carriers, the research ranges from the production to direct use of the carriers. Prior to his current role, he led the chemical technology R&D department at Linde Engineering. He made significant contributions to numerous publications and patents concerning the innovative design, operation, and control of chemical and process plants.

ABSTRACT

Hydrogen carriers, such as dimethyl ether (DME), offer a promising path toward carbon-neutral power generation and the development of a hydrogen-based energy economy. DME has the potential to address the uneven regional and temporal distribution of renewable energy by enabling long-distance energy transfer. Furthermore, its favorable combustion characteristics and compatibility with existing infrastructure position DME as an attractive renewable fuel.

This study aims to comprehensively compare the performance of DME as a fuel in advanced oxy-combustion supercritical CO_2 (sCO_2) cycles, such as the Allam cycle, and in state-of-the-art combined cycle gas turbines with post-combustion carbon capture (CCGT-PCC). In addition to the reference Allam cycle, we propose a novel modification: the Liquefied Recycle Allam Cycle (LiRAC). This modification features an integrated refrigeration unit that enables liquefaction of the working medium using DME as the refrigerant. Process simulations demonstrate that the LiRAC achieves a competitive efficiency of 48.7 %, approaching that of the DME-fueled Allam cycle (50.4 %), with both cycles achieving effective carbon capture rates above 96 %, approaching carbon neutrality. However, under consistent system boundaries, the DME-fueled CCGT-PCC achieves an efficiency of only 44.7 %. These findings demonstrate the feasibility of using DME as a fuel for semi-closed oxy-combustion sCO_2 cycles and highlight its potential as a pathway toward nearly carbon-neutral power generation.

INTRODUCTION

As electricity demand rises due to increased electrification, maintaining a stable energy supply becomes essential. Although expanding renewable energy sources is important, the uneven distribution of these sources across regions and over time means that future energy systems must enable long-distance energy transfer and ensure grid stability. Thermal power plants can play a vital role in addressing the rapid growth of electrification while ensuring grid stability and supply. Specifically, chemical energy carriers, such as dimethyl ether (DME) produced from carbon dioxide and green hydrogen in regions with abundant renewable energy, enable the on-demand generation of heat and electricity in regions that consume more energy than they produce. Due to its high energy density, DME can be transported as a hydrogen derivative to consumer regions, where it can serve two purposes: it can be used directly as a fuel due to its good combustion properties, and it can serve as a hydrogen carrier from which hydrogen can be extracted through reforming.

Ensuring a sustainable path requires capturing most of the CO_2 generated when either using DME for power generation or for H_2 production. Transporting DME and captured CO_2 in the same vessel offers an attractive pathway toward sustainable CO_2 deployment and securing the CO_2 feedstock for DME synthesis. For power generation, the challenge becomes finding the right power generation cycle. This cycle must be able to achieve high capture rates with attractive efficiencies. The captured CO_2 should also align with the International Organization for Standardization (ISO) standards for transportation [1,2]. This will enable standardized CO_2 deployment.

The state-of-the-art power generation technology is a combined cycle gas turbine with a chemical solvent-based post-combustion carbon capture system (CCGT-PCC). However, emerging supercritical carbon dioxide (sCO_2) oxy-combustion technologies, such as the Allam cycle, provide an alternative, integrated approach to traditional post-combustion capture (PCC). The Allam cycle has a high technology readiness level among sCO_2 power cycles and demonstrates competitive efficiency when natural gas is used as fuel. Additionally, using sCO_2

as a working medium in power cycles is expected to yield favorable economic outcomes, primarily due to compact equipment [3].

In this study, we examine the dimethyl ether (DME)-fueled Allam cycle and present a new cycle configuration: the Liquified Recycle Allam Cycle (LiRAC). In the LiRAC, a vapor compression unit (VCU) with DME as the refrigerant is integrated into the process. The oxy-combustion processes are further benchmarked to a DME-fueled CCGT-PCC with the same CO_2 product specifications, considering the impact of high capture rates and purification on the overall efficiency. The Allam cycle, the LiRAC cycle, and the CCGT-PCC cycle are coupled with a compression and purification unit (CPU) to achieve the CO_2 purity required by ISO standards for pipeline transportation. The simulations and the aligned system boundaries enable a comparative analysis of all cycles.

SYSTEMS DESCRIPTION

This study examines three simulated power generation cycles fueled both by DME: two oxy-combustion cycles (the Allam cycle and the LiRAC) and a conventional combined cycle gas turbine process with post-combustion carbon capture. Each cycle is coupled with a CPU to purify and condition the captured CO_2. This study does not address the details of the CPU models, focusing instead on the overall performance of the power cycles. All cycles were simulated with a fixed thermal input of 1536 MWth (LHV basis) to enable direct comparison.

Combined Cycle Gas Turbine with Post-Combustion Carbon Capture (CCGT-PCC)

Unlike the Allam cycle, the CCGT-PCC cycle is regarded as a state-of-the-art power generation technology suitable for near-term implementation, making the CCGT-PCC a useful reference. Figure 1 illustrates the process flow diagram of the modeled DME-fueled CCGT. Consistent with the literature [4,5], the cycle consists of a gas turbine that operates at an inlet temperature of 1,500 °C and a pressure ratio of 15. The heat contained in the turbine exhaust gases is recovered in a bottoming steam-Rankine cycle before the exhaust stream is directed to a PCC unit for CO_2 recovery and subsequent conditioning in a CPU.

The bottoming steam-Rankine cycle includes a heat recovery steam generator (HRSG) with high-pressure (HP), intermediate-pressure (IP), and low-pressure (LP) steam, as well as their respective superheaters, reheaters, evaporators, economizers, turbines, and pumps.

The condensed water from the condenser (13) is pressurized and preheated in the HRSG and mixed with some of the LP steam in the deaerator (5). Booster pumps then pressurize the feedwater to the respective pressure levels. The HP steam is superheated to 600 °C at 170 bar and expanded in the HP turbine. Steam from the HP turbine is recirculated to the HRSG, where it combines with IP superheated steam and is reheated to 600 °C. Then, the IP hot steam expands within the IP turbine. Superheated LP steam is introduced at the IP/LP crossover before entering the last turbine. The steam subsequently expands through the LP turbine to the condenser pressure. The steam is then supplied to the reboiler of the PCC plant from the IP/LP crossover.

To assess the energy demand required for the PCC plant's chemical solvent process, we used a simplified model. The steam extracted from the Rankine cycle (see Figure 1) undergoes desuperheating to a temperature of 153 °C, and the mass flow is calculated based on the PCC plant's assumed recovery rate of 99 % and the specific reboiler duty (SRD) value. The SRD value was scaled from a

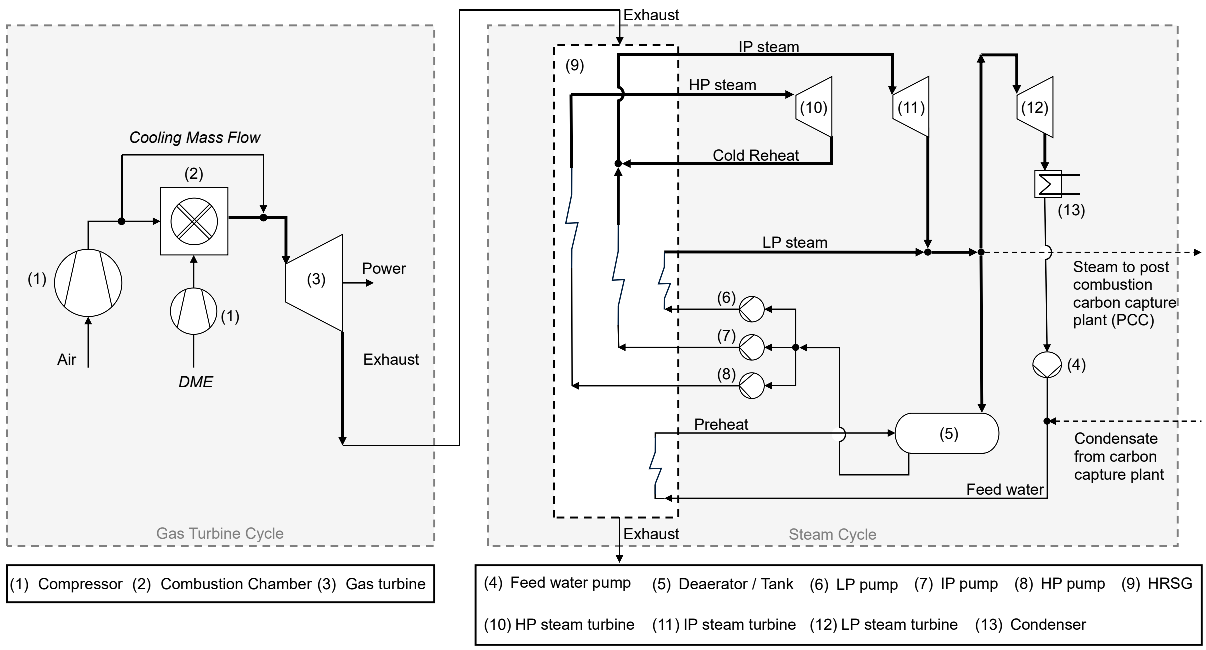

Figure 1: Simplified process flow diagram of the simulated combined cycle gas turbine (CCGT).

baseline of 2.9 GJ t^{-1} at a 90 % recovery rate [6], resulting in a 26 % increase to 3.665 GJ t^{-1} at a 99 % recovery rate [7]. To account for impurities in the recovered CO_2 from the PCC plant, we assume that the CO_2 stream directed to the CPU contains non-condensable gases up to the maximum concentration permitted for enhanced oil recovery (EOR) applications (i.e., up to 100 ppm mol of oxygen).

DME-fueled Allam Cycle

Various configurations of the Allam cycle have been reported in literature and patents, with differing levels of technical detail. In this study, the Allam cycle is modeled according to the works of the IEAGHG and Scaccabarozzi et al. [8,9]. Figure 2 and Figure 3 illustrate the process flow and the corresponding temperature-entropy diagrams, respectively.

DME (stream 1) is combusted in the presence of an oxidant stream and a CO_2 diluent to regulate the temperature of the combustor at 1,150 °C. The combustion process operates with a 3 % excess of oxygen relative to the stoichiometric ratio, using high-purity oxygen (99.5 mol%) supplied from an air separation unit (ASU) at 120 bar and 15 °C. In this study, the ASU is represented by a specific energy demand of 1390 kJ kg^{-1} O_2 and a stream of hot air [8].

The combustion products (stream 4, Figure 2), primarily composed of CO_2 and H_2O, expand through the turbine to a pressure of 34 bar. The expanded stream is then cooled in a recuperator where residual heat is recovered and transferred to the high-pressure streams entering the combustor. Additionally, hot air from the ASU compressors provides supplementary heat to the system via the recuperator.

After the recuperator, stream 6 is cooled further to 26 °C to enable the condensation and separation of water. A portion of the stream is directed to the compression and purification unit for integrated carbon capture. The remaining stream is compressed and cooled in four intercooled stages to 100 bar, beyond the critical point. Then, it is cooled to 26 °C to achieve a dense phase before being pumped to 120 bar (stream 8).

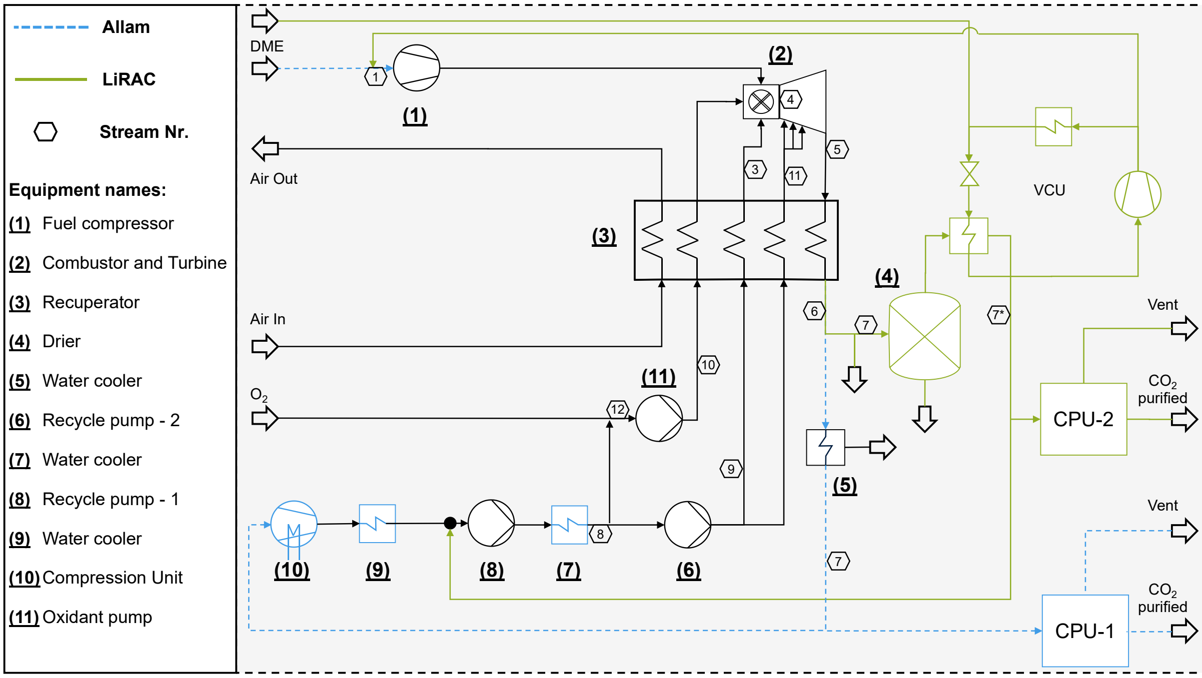

Figure 2: Simplified process flow diagrams of the simulated Allam and LiRAC cycles. The blue dotted lines represent the Allam cycle while the green lines represent the LiRAC. The black lines are common to both cycles.

A portion of this stream is mixed with oxygen to form an oxidant mixture (stream 10) with 13.34 mol % O_2. The oxidant and the remaining part of the recycled stream are pressurized further by separate pumps to a maximum pressure of 305 bar (streams 9 and 10). Then, they undergo preheating before entering the combustor.

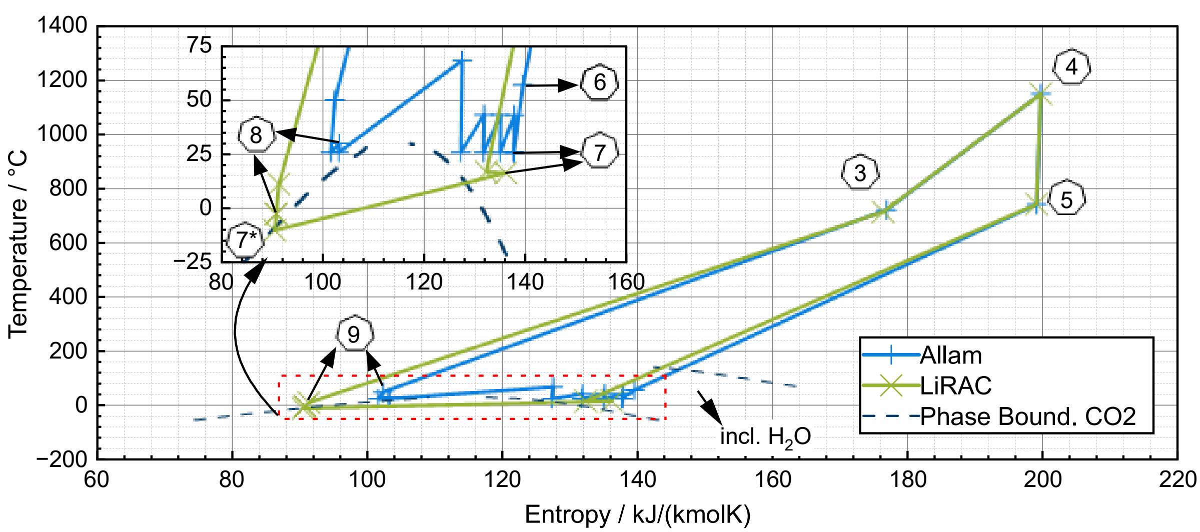

Figure 3: Temperature-entropy diagram of the simulated Allam and LiRAC cycles.

Liquified Recycle Allam Cycle (LiRAC)

The LiRAC cycle is a modified Allam cycle in which the recycled stream is liquefied using an integrated VCU (see Figure 2 and Figure 3). In this study, the LiRAC and Allam cycles are modeled under the same assumptions and process parameters.

A pivotal step in the Allam cycle is compressing the recycled stream beyond the critical point, followed by further cooling to achieve the dense phase. However, this step is highly sensitive to the critical point of the mixture.

Unlike the Allam cycle, the LiRAC uses subcritical liquefaction of the recycled stream at the lowest cycle pressure. This allows the entire pressurization to be achieved solely through pumping. This configuration ensures a dense phase at the pump inlet, independent of the critical point. Thus, it is more robust against small variations in the recycle stream composition.

From a process perspective, the modification begins with the partially condensed exhaust gas from the recuperator (stream 6, Figure 2). After the water is removed, the exhaust gas (stream 7) is dried to prevent ice formation during liquefaction. Then, the dried gas is liquefied using the VCU (stream 7*). A portion of the liquid stream is extracted and sent to the CPU. The rest is recycled and pressurized by pumps instead of compressors, eliminating the intercooled compression unit and simplifying the pressurization process.

A distinctive feature of the LiRAC configuration is the ability to integrate a raw liquid CO_2 buffer tank at stream 7*. This tank decouples the CPU, VCU, and power cycle, potentially enabling smoother operation, improved part-load flexibility, and controlled CO_2 handling.

Figure 4 illustrates the VCU's process flow and corresponding pressure-enthalpy diagrams. The refrigerant of the VCU is the fuel DME, so the fuel is first given to the refrigerant loop of the VCU as a liquid at 26 °C. The refrigerant (stream III, Figure 4) undergoes recuperative subcooling before being throttled to 1.79 bar and -12 °C (stream IV), ensuring the necessary temperature difference in the evaporator. After the evaporator, the refrigerant is superheated and compressed. After compression, the fuel is extracted and supplied to the fuel compressor of the power cycle. The remaining refrigerant is then recycled within the VCU loop.

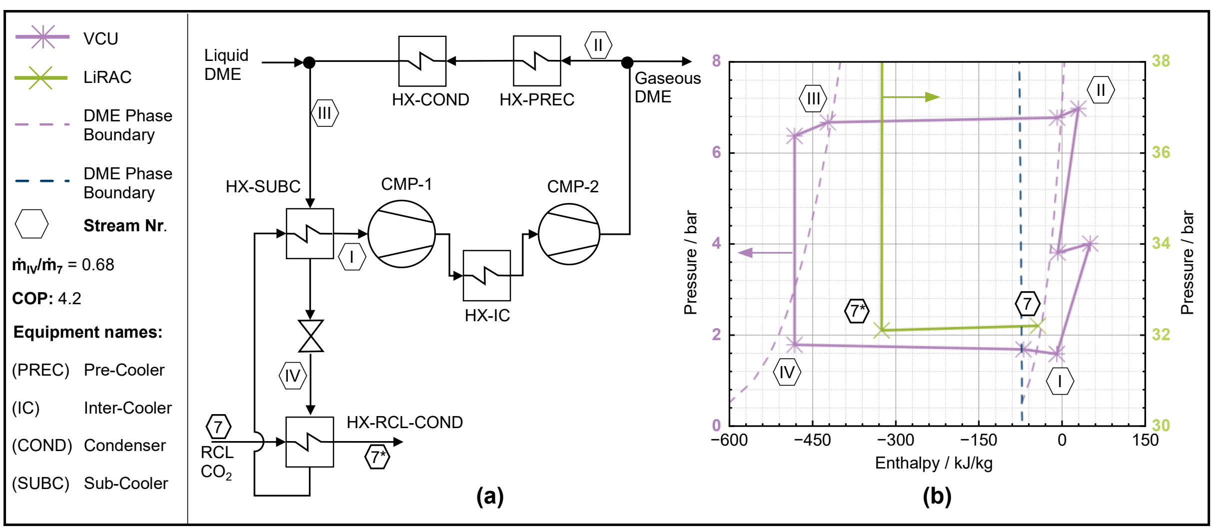

Figure 4: (a): Simplified process flow diagram of the VCU. (b): Pressure enthalpy diagram of the VCU

MODELING AND EVALUATION METRICS

This section describes the modelling approach adopted in this study to evaluate the performance of the power cycles. The metrics used for evaluation are also listed and described.

Modeling

All cycles were simulated using steady-state process models modeled in the software AVEVA® Process Simulation (APS). Mass and energy balances were solved using built-in models. The Peng-Robinson equation of state was applied to the Allam cycle and LiRAC, consistent with prior studies [9] and in-house density validation against experimental data. For the CCGT-PCC, the Soave-Redlich-Kwong (SRK) equation of state was applied to the gas turbine model following Jonsson et al. [10], while the Rankine cycle was modeled using the IAPWS-IF97 steam tables.

Evaluation metrics

This work uses three metrics to compare the technical and environmental performance of the cycles. The first is net efficiency, defined as the ratio of net electrical output to total thermal input on an LHV basis, as in Eq.{1}.

$$\eta_{\mathrm{net}} = \frac{P_{\mathrm{net}}}{\dot{m}_{\mathrm{fuel}} * LHV} \qquad \{1\}$$

Second is the carbon capture rate (R_{CC}), which is defined as the ratio of captured, purified, and pipeline-ready CO_2 to the total mass flow of CO_2 imported and generated (cf. Eq. {2}).

$$R_{CC} = \frac{\dot{m}_{\mathrm{CO2,purified}}}{(\dot{m}_{\mathrm{CO2,input,air}})_{\mathrm{CCGT}} + \dot{m}_{\mathrm{CO2,fuel,stoich}}} \qquad \{2\}$$

The mass flow of CO_2 accounted for the fuel (cf. Eq. {3}), includes the minor share of CO_2 present in the fuel input and the CO_2 generated through combustion.

$$\dot{m}_{\mathrm{CO2,fuel,stoich}} = \dot{m}_{\mathrm{CO2,generated}} + \dot{m}_{\mathrm{CO2,input,fuel}} \qquad \{3\}$$

Third is the CO_2 emission intensity, which provides a measure of environmental performance by relating all direct CO_2 emissions to the net power output. (cf. Eq. {4}). Emissions include CO_2 from the conditioning system (vent), stack emissions from the PCC plant, and dissolved CO_2 in condensate. For the CCGT, CO_2 contained in the air intake is considered a negative term.

$$CO_2 \text{ emission intensity} = \frac{(\dot{m}_{\mathrm{CO2,stack,amine\ wash}})_{\mathrm{CCGT}} + \dot{m}_{\mathrm{CO2,vent,CPU}} + \dot{m}_{\mathrm{CO2,dissolved}} - (\dot{m}_{\mathrm{CO2,input,air}})_{\mathrm{CCGT}}}{P_{\mathrm{net}}} \qquad \{4\}$$

RESULTS AND DISCUSSION

The processes under consideration were analyzed based on their net efficiency, carbon capture rate, and CO_2 emission intensity. The results are discussed and contextualized below.

Comparative Analysis of Oxy-Combustion sCO_2 Cycles vs. CCGT-PCC

This section compares the Allam and the LiRAC against the state-of-the-art CCGT-PCC power generation cycle. To ensure a fair comparison, the system boundaries were aligned. The CCGT-PCC is consequently designed for a 99 % CO_2 recovery rate and additional conditioning through a CPU to achieve the same product specifications as the oxy-combustion systems. A summary of the key performance indicators (KPIs) is provided in Table 1. The findings indicate that oxy-combustion outperforms the CCGT-PCC. When considering carbon capture and conditioning, the CCGT-PCC achieves a net efficiency of only 44.7 %, which is 5.7 % lower than the Allam and 4 % lower than the LiRAC. Even when excluding the CPU's power demand, the Allam cycle maintains an efficiency advantage. This suggests that the energy demand of the solvent-based carbon capture significantly impacts efficiency even without further CO_2 conditioning. All cycles achieved effective capture rates of approximately 96 %.

Overall, the results show that sCO_2 power cycles are more efficient than CCGT-PCC cycles when the same boundary conditions are used for comparison. The outcomes positions sCO_2 power cycles as a promising technology for power generation.

Table 1: Performance summary of the simulated cycles

Process		**LiRAC**	**Allam**	**CCGT-PCC**
Parameter	**Unit**	**Energy performance**		
Net efficiency	%	48.7	50.4	44.7
Net efficiency excl. CPU	%	49.4	53.5	50.8
El. net power output	MWe	748.5	774.8	687.3
CPU Power consumption	MWe	10.2	46.9	93.2
		CC rate and CO_2 emission intensities		
Recovery rate (CPU)	%	98.9	98.9	97.5
Effective CC rate	%	96.0	96.6	96.5
CO_2 emission intensity	kg/MWh	19.6	16.1	15.5
CO_2 emission intensity excl.CO_2 dissolved	kg/MWh	5.2	5.1	15.5
		Essential mass flows		
Fuel mass flow	kg/s	53.2	53.2	53.2
CO_2 purified	kg/s	97.7	98.4	98.9
CO_2 input (air, fuel and CO_2 generated)	kg/s	101.8	101.8	102.4
CO_2 dissolved	kg/s	3.0	2.4	0.0
CO_2 emissions (Vent and Stack)	kg/s	1.1	1.1	3.6

Energy Breakdown of the Allam Cycle vs. the LiRAC

Figure 5 illustrates the energy consumption and production of the Allam and LiRAC equipment.

Both cycles demonstrate high efficiency on an energy basis, with 50.4 % for the Allam and 48.7 % for the LiRAC. The LiRAC turbine delivers 15.3 MW less mechanical power than the Allam cycle turbine, primarily due to the lower recuperator outlet temperature (see Figure 5). The lower input temperature at the combustor inlet results in a reduced recycled mass flow rate to reach the desired combustor outlet temperature, which lowers the turbine mass flow and consequently the turbine power output. Additionally, the integrated VCU compressor in the LiRAC requires 176 MWe, yielding a coefficient of performance of 4.2. This is higher than the recycle compressor's power demand in the Allam cycle (130.8 MWe). This difference primarily results from the VCU compressors' higher pressure ratio (4.4) compared to the recycle compressors' (3.05). In contrast, the CPU in the LiRAC requires less power demand (10.2 MWe) than the CPU in the Allam cycle (46.9 MWe). The difference is attributed to the liquid feed of the CPU in the case of LiRAC. The liquid state lowers the energy demand for the liquefaction in the CPU.

Overall, these results suggest that DME is a promising fuel for sCO_2 oxy-combustion power cycles. With an efficiency that is only 1.7 % lower than that of the Allam cycle, the LiRAC demonstrates feasibility while potentially offering a simpler pressurization concept through liquid-phase pumping.

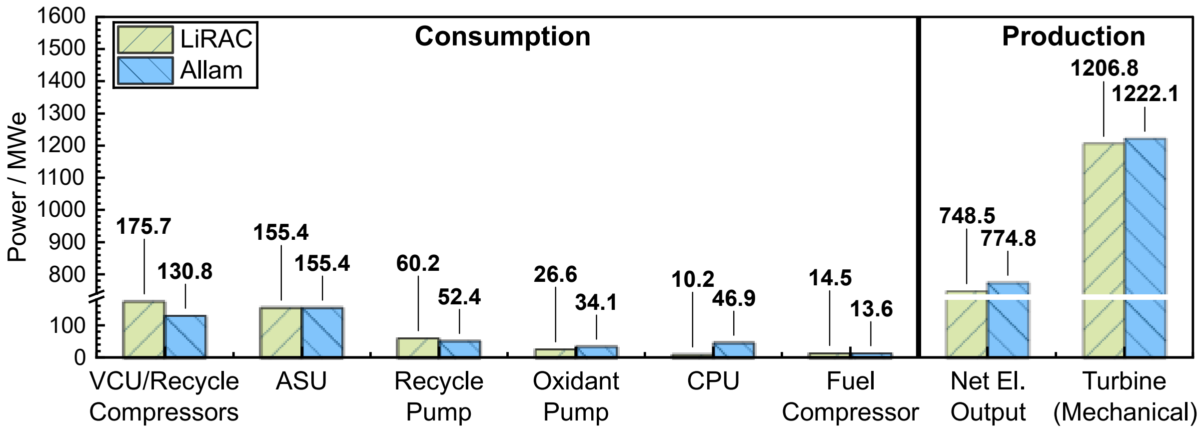

Figure 5: Energy breakdown for the Allam and LiRAC cycles.

CONCLUSION

In this study, we present a detailed, simulation-based performance assessment of DME-fueled oxy-combustion power cycles, including rigorous benchmarking against a conventional combined cycle gas turbine. We also introduce the Liquefied Recycle Allam Cycle (LiRAC), a promising modification of the Allam cycle that incorporates a vapor compression unit with DME as the refrigerant. Results indicated high overall efficiencies of 50.4 % for the Allam cycle and 48.7 % for the LiRAC cycle, with effective carbon capture rates of 96 %, approaching carbon-neutral power generation. For reference, we simulated a state-of-the-art DME-fueled CCGT-PCC power cycle under equivalent boundary conditions, including high CO_2 recovery and purification. The results showed that the oxy-combustion cycles clearly outperformed. Nevertheless, the primary benefit of CCGT-PCC is still the advanced technology readiness and retrofit potential for existing plants. The captured CO_2 in all cycles meets the oxygen impurity limit of less than 10 ppm mol and is fully prepared for pipeline transportation. This enables direct deployment and a nearly closed carbon loop when the captured CO_2 is reused for DME synthesis. The narrow efficiency gap between the Allam and LiRAC cycles confirms the feasibility of the modification. Therefore, further work should focus on optimizing and analyzing part loads to fully explore the potential of the LiRAC cycle.

ACKNOWLEDGEMENTS

The authors acknowledge the funding by the German Federal Ministry of Research, Technology and Space and the Ministry of Economic Affairs, Industry, Climate Action and Energy of the State of North Rhine-Westphalia through the project HC-H2.

References

[1] ISO 27913. Carbon dioxide capture, transportation and geological storage - Pipeline transportation systems; 2024.
[2] ISO/TR 27929. Transportation of CO_2 by ship; 2024.
[3] Klaus Brun, Peter Friedman, Richard Dennis (eds.). Fundamentals and Applications of Supercritical Carbon Dioxide (sCO_2) Based Power Cycles. Woodhead Publishing; 2017.
[4] IEAGHG. CO_2 Capture at Gas Fired Power Plants, 2012/8, July, 2012.
[5] IEAGHG. Retrofit of CO2 Capture to Natural Gas Combined Cycle Plants. Report Number 2005 / 1 2005.
[6] M. Turner, T. Schmitt, M. Oakes, J. Konrade, M. Bleckinger, M. Sturdivan. Cost and Performance Baseline for Fossil Energy Plants. Volume 3: Low Rank Coal and Natural Gas to Electricity. Pittsburgh; 2023.

[7] IEAGHG. Update techno-economic benchmarks for fossil fuel-fired power plants with CO_2 capture, 2020/07, July 2020.
[8] IEAGHG. Oxy-Combustion Turbine Power Plants, 2015/05, August, 2015.
[9] Scaccabarozzi R, Gatti M, Martelli E. Thermodynamic analysis and numerical optimization of the NET Power oxy-combustion cycle. Applied Energy 2016;178:505–26. https://doi.org/10.1016/j.apenergy.2016.06.060.
[10] Maria Jonsson, Olav Bolland, Dominikus Bücker, Miker Rost. Gas turbine cooling model for evaluation of novel cycles. In: Proceedings of ECOS 2005.